

Mechanism of Acid-Catalyzed Epoxidation of Alkenes with Peroxy Acids

Robert D. Bach,^{*,1a} Carlo Canepa,^{1a} Julia E. Winter,^{1b} and Paul E. Blanchette^{1b}

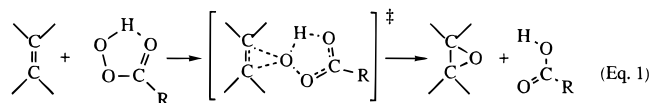
Department of Chemistry and Biochemistry, University of Delaware, Newark, Delaware 19716 and
Department of Chemistry, Wayne State University, Detroit, Michigan 48202

Received May 22, 1995[©]

A 6.8 fold increase in the rate of epoxidation of (*Z*)-cyclooctene with *m*-chloroperbenzoic acid is observed upon addition of the catalyst trifluoroacetic acid. Kinetic and theoretical studies suggest that this increase in rate is due to complexation of the peroxy acid with the undissociated acid catalyst (HA) rather than protonation of the peroxy acid. The transition structure for oxidation of ethylene with protonated peroxyformic acid exhibits a spiro orientation of the electrophilic oxygen at the QCISD/6-31G(d) level and the complexed peroxy acid (HCO₃H·HA) transition state is also essentially spiro at the *ab initio* and density functional levels. At the B3LYP/6-311G(d,p) level the protonated transition structure exhibits a more planar approach where the O₃-H₉ of the peroxy acid lies in the plane of the π-system of ethylene, and the barrier for formation of protonated oxirane is only 4.4 kcal mol⁻¹. Epoxidation with neutral and complexed peroxyformic acid also involves a symmetrical spiro orientation affording an epoxide, and the barriers for formation of oxirane at the same level are 14.9 kcal mol⁻¹ and 11.5 kcal mol⁻¹, respectively. The free energy of activation for the epoxidation of ethylene by peroxyformic acid is lowered by about 3 kcal mol⁻¹ upon complexation with the catalyst.

Introduction

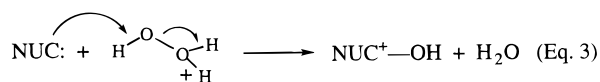
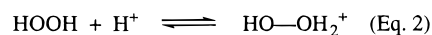
Despite the development of many new oxidation procedures, the use of peroxy acids still constitutes a useful synthetic procedure for the epoxidation of alkenes on a laboratory scale.² Oxygen atom transfer from a peroxy acid to an alkene is facilitated by electron-donating substituents on the carbon-carbon double bond and electron-withdrawing groups on the peroxy acid.³ The commonly accepted mechanism for oxirane formation involves a cyclic polar process where the proton is transferred intramolecularly to the carbonyl oxygen with simultaneous attack by the alkene π-bond. This concerted process was suggested initially by Bartlett,⁴ and because of the unique planar transition structure (TS) it is often referred to as the "butterfly" mechanism (eq 1).



On the basis of earlier theoretical studies we suggested that the nucleophilic π-bond of the alkene attacks the O-O σ bond in an S_N2 fashion with displacement of a neutral carboxylic acid.⁵

While a protonated peracid should be a much more effective oxygen atom donor than its neutral counterpart,

experimentalists have reported only a modest rate enhancement for acid-catalyzed epoxidation. This is especially puzzling when consideration is given to the activating influence of strong acid on the reactivity of H₂O₂. It has been shown that the rate of oxidation may be increased by at least two powers of ten and that this occurs by a two-step process involving specific acid catalysis (eqs 2, 3).²



Indeed, Olah and co-workers have successfully achieved hydroxylation of branched chain saturated hydrocarbons in "magic acid" media containing FSO₃H.⁶

Early attempts to effect acid catalysis in alkene epoxidation, where relatively weak acids such as benzoic acid were employed, proved unsuccessful.⁷ In addition, no acid catalysis was observed in the perbenzoic acid epoxidation of cyclohexene upon addition of dichloroacetic acid in a benzene-ether solvent system.^{3d} This situation was further complicated by contradictory data concerning the influence of addition of acids on epoxidation rates.^{3b,8} Trichloroacetic acid catalyzes the rate of epoxidation of stilbene with perbenzoic acid but retards the rate of epoxidation of a double bond bearing an ester substituent like in ethyl crotonate.^{3b,8} In an early study on the oxidation of sulfides with peroxybenzoic acid Modena established a modest catalysis by trifluoroacetic acid in carbon tetrachloride and benzene solvent but not in

[©] Abstract published in *Advance ACS Abstracts*, June 15, 1997.

(1) (a) University of Delaware; E-mail rbach@udel.edu; WWW http://www.udel.edu/chem/bach. (b) Wayne State University.

(2) Edwards, J. O. *Peroxide Reaction Mechanisms*; Edwards, J. O., Ed.; Interscience: New York, 1962; pp 67–106.

(3) (a) Lynch, B. M.; Pausacker, K. H. *J. Chem. Soc.* **1955**, 1525. (b) Schwartz, N. N.; Blumbergs, J. H. *J. Org. Chem.* **1964**, *29*, 1976. (c) Vilka, M. *Bull. Soc. Chim. Fr.* **1959**, 1401. (d) Renolen, P.; Ugelstad, J. *J. Chim. Phys.* **1960**, *57*, 634. (e) House, H. O.; Ro, R. S. *J. Am. Chem. Soc.* **1958**, *80*, 2428. (f) Ogata, Y.; Tabushi, I. *J. Am. Chem. Soc.* **1961**, *83*, 3440, 3444. (g) Curci, R.; Di Prete, R. A.; Edwards, J. O.; Modena, G. *J. Org. Chem.* **1970**, *30*, 740.

(4) Bartlett, P. D. *Rec. Chem. Progr.* **1950**, *11*, 47.

(5) (a) Bach, R. D.; Willis, C. L.; Domagals, J. M. *Applications of MO Theory in Organic Chemistry*; Csizmadia, I. C., Ed.; Elsevier Scientific: Amsterdam, 1977; Vol. 2, p 221. (b) Bach, R. D.; Andrés, J. L.; Davis, F. *J. Org. Chem.* **1992**, *57*, 613.

(6) Olah, G.; Parker, D. G.; Yoneda, N. *Angew Chem., Int. Ed. Engl.* **1978**, *17*, 909.

(7) Campbell, D. R.; Edwards, J. O.; MacLachlan, J.; Polgar, K. *J. Am. Chem. Soc.* **1958**, *80*, 5308.

(8) (a) Berti, G.; Botturi, F. *Gazz. Chim. Ital.* **1959**, *89*, 2380. (b) Berti, G.; Botturi, F. *J. Org. Chem.* **1960**, *25*, 1286.

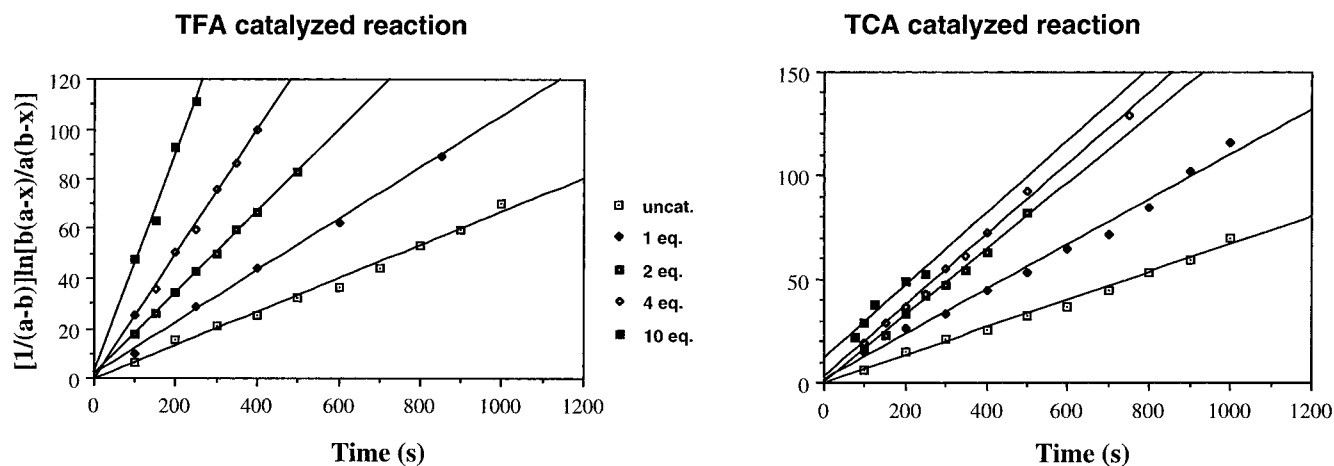


Figure 1. Second-order rate expression for the epoxidation of (*Z*)-cyclooctene with MCPBA in the presence of 0, 1, 2, 4, and 10 equiv of trifluoro- and trichloroacetic acid. $a = [\text{peracid}]_{t=0}$, $b = [\text{alkene}]_{t=0}$, $x = [\text{epoxide}]$. The slope of the lines is given by $k_{\text{obs}} = k_0 + k_{\text{cat}}K_{\text{eq}}[\text{HA}]$, where K_{eq} is the equilibrium constant for the formation of cluster-9.

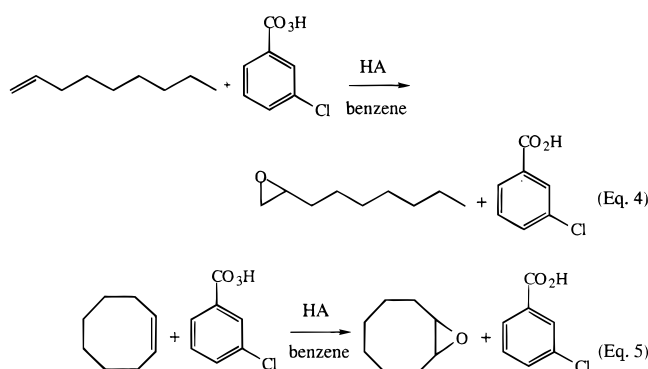
dioxane.^{9a} A subsequent kinetic study by Sapunov and Lebedev^{9b} also served to clarify some of these discrepancies. They observed about a ten-fold increase in the rate of epoxidation of allyl chloride in the presence of 0.5 M perchloric acid ($\text{p}K_{\text{a}} = -10$). They found that this reaction is first order with respect to both peracid and protic acid. The rate of epoxidation increased with increasing acid strength and decreased with increasing basicity of the solvent. For example, the catalytic effect was maximized in weakly basic solvents like benzene, chloroform, and chlorobenzene and the relative rates in all three solvents were approximately the same. However, in solvents that possess a more basic carbonyl group, the catalytic effect was dramatically retarded thereby confirming the apparently conflicting data above. The dielectric constant of the solvent does not play a dominant role since the charge separation in the TS is effectively reduced by the intramolecular hydrogen transfer.

Results and Discussion

Experimental Studies. The objective of the experimental part of this study¹⁰ was to provide a quantitative assessment of the rate acceleration of epoxidation of simple alkenes with acids of moderate acidity such as trichloro- and trifluoroacetic acid. One of the problems associated with realizing the benefits of acid catalysis is the lack of stability of the oxirane products in the presence of strong acids.

We initiated a kinetic study of the epoxidation of 1-nonene with *m*-chloroperbenzoic acid (MCPBA) in the presence of either CCl_3COOH (TCA) or CF_3COOH (TFA) in benzene solvent. Reactions were carried out under pseudo-first-order conditions with the alkene present in at least a ten-fold excess. Reaction rates were monitored by following the formation of 1,2-epoxynonane by gas phase liquid chromatography (eq 4). However, this protocol was flawed due to the acid catalyzed decomposition of the epoxide product. As a result of control experiments that established the rate of epoxide decomposition we did estimate a 3.4 and 4.7 fold rate increase in epoxidation rate in the presence of 10 equiv of TCA ($\text{p}K_{\text{a}} = 0.9$) and TFA ($\text{p}K_{\text{a}} = 0.2$) relative to the uncatalyzed oxidation.

To alleviate the problem of epoxide ring opening under the conditions of the kinetic studies, (*Z*)-cyclooctene was



used as the alkene (eq 5). Control experiments established a loss of only 4.7% cyclooctene oxide when stirred in the presence of 10 equivalents of TFA for 1 h. This time period is far in excess of the half-life of the uncatalyzed reaction ($t_{1/2} = 855$ s). The increased stability of cyclooctene oxide to acid-catalyzed decomposition is presumably due to increased transannular interactions in the transition structure for nucleophilic attack on the protonated oxirane intermediate. The use of (*Z*)-cyclooctene did impose one additional problem due to its increased nucleophilicity relative to 1-nonene. For example, a disubstituted alkene such as cyclohexene reacts 27 times faster than the monosubstituted alkene 1-hexene.¹¹ A plot of the second-order rate expression versus time is given in Figure 1.

Examination of second-order rate constants demonstrate a modest increase in the rate of oxygen atom transfer from MCPBA to (*Z*)-cyclooctene upon acid catalysis. With 10 equiv of TCA and TFA a 4.0 and 6.8 fold increase in the rate of reaction was observed relative to the uncatalyzed reaction. A much smaller increase (1.4 fold) was noted for 10 equiv of acetic acid ($\text{p}K_{\text{a}} = 4.7$). Even with 20 equiv of acetic acid only a 1.5 fold rate enhancement was noted. The observed second-order rate constants (k_2) for the catalyzed reactions (10 equiv of

(9) (a) Modena, G.; Todesco, P. E. *J. Chem. Soc.* **1962**, 4920. (b) Sapunov, V. N.; Lebedev, N. N. *Zh. Org. Khim.* **1966**, 2, 225. (c) Valov, P. I.; Blyumberg, E. A.; Filippova, T. V. *Kinet. Catal. (Transl. of Kinetika i Katal.)* **1967**, 8, 760.

(10) Blanchette, P. A. Wayne State University, Masters Thesis, 1979.

(11) (a) Swern, D. *J. Am. Chem. Soc.* **1947**, 69, 1692. (b) The relative rates of epoxidation of ethene, propene, styrene, isobutene, and 2-butene with peracetic acid are 1, 22, 59, 484, and 489, respectively.

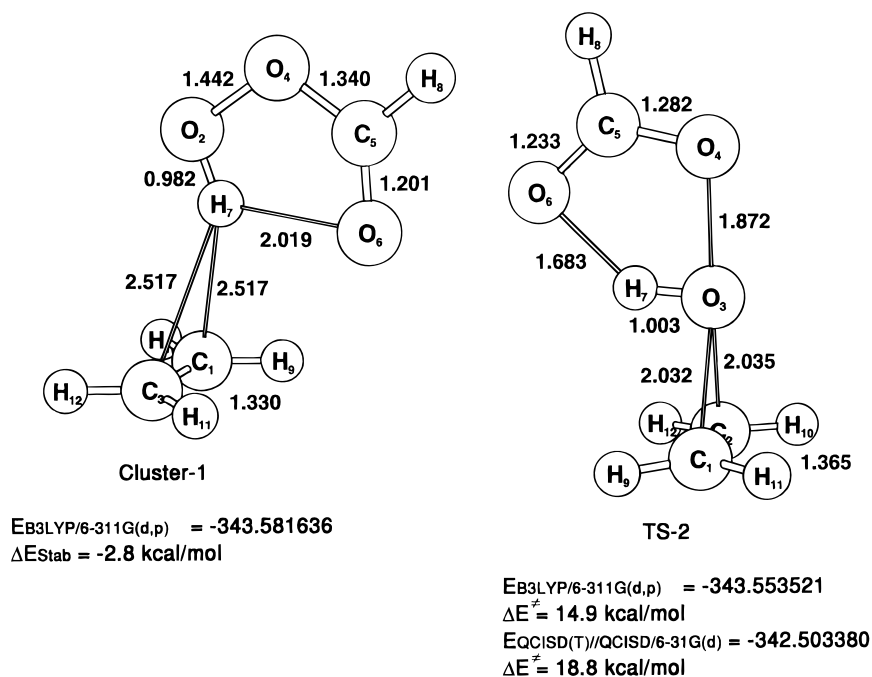


Figure 2. Peroxyformic acid–ethylene cluster (1) and its transition structure for epoxidation (TS-2) optimized at B3LYP/6-311G(d,p). Total energies are in Hartrees, distances in angstroms, and angles in degrees. The energy of ethylene and peroxyformic acid at the level indicated are -78.613977 and -264.963266 , respectively. The activation barrier is calculated from isolated reactants.

acid) are 0.092 ± 0.010 , 0.266 ± 0.003 , and 0.453 ± 0.012 $\text{M}^{-1} \text{s}^{-1}$ for acetic acid, TCA, and TFA, respectively, using the rate expression:

$$-\frac{d[\text{peracid}]}{dt} = k_2[\text{alkene}][\text{peracid}] \quad (\text{eq } 6)$$

In the Sapunov and Lebedev^{9a} kinetic study the observed rate constant is given by:

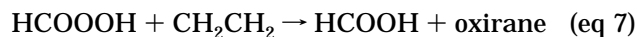
$$k_2 = k_0 + k_{\text{HA}}[\text{HA}]$$

where HA is the strong acid catalyst. These data are consistent with the minimal protic acid catalysis that earlier workers observed with relatively weak acids such as benzoic acid ($\text{p}K_{\text{a}} = 4.2$). The corresponding uncatalyzed reaction exhibits a rate constant of 0.0665 ± 0.0002 $\text{M}^{-1} \text{s}^{-1}$.

It remained to be shown that the modest rate increase was attributable to the protic acid and not due to an increase in polarity of the reaction medium as a consequence of added acid to the system. To test the potential role of an increase in dielectric constant on the rate of epoxidation, 10 equiv of 2,2,2-trifluoroethanol were added in place of the acid catalyst. We note a rate increase of about 10% which tends to exclude any major contribution of the dielectric constant on the rate of epoxidation. In order to understand this level of catalytic activity we undertook a computational study to examine the overall mechanistic pathway for alkene epoxidation.

Computational Studies. The *ab initio*¹² and Density Functional Theory (DFT) calculations¹³ that we have performed on simple alkenes suggest that a spiro transition structure, where the C–C bond axis and the plane of the peroxy acid moiety are at right angles (TS-2, Figure 2), is slightly favored over a planar “butterfly”. The “electrophilic” oxygen atom attacks the center of the alkene π -bond, affording a symmetrical TS with a spiro orientation of the reactants.¹⁴ A recent *ab initio* study

of the parent reacting system (eq 7) at the MP2 level



suggested an unsymmetrical approach of the electrophilic oxygen over one carbon atom of the double bond of ethene.¹⁵ A transient intermediate lying on the reaction pathway between the transition structure and a protonated oxirane–formate anion complex was also located at the MP2 level. Our data at the CCSD(T) level suggest that these findings are an artifact of the MP2 method.¹⁴ The activation barriers for alkene epoxidation calculated at the B3LYP/6-31G(d) and B3LYP/6-31+G(d) levels are systematically lower (5–6 kcal/mol) than the barrier heights calculated at such more highly correlated levels as QCISD(T)/6-31G(d), CCSD(T)/6-31G(d)//CCSD/6-31G-

(12) (a) Theoretical calculations were carried out using the Gaussian94 program system^{12b} utilizing gradient geometry optimization. (b) Frisch, M. J.; Trucks, G. W.; Schlegel, H. B.; Gill, P. M. W.; Johnson, B. G.; Robb, M. A.; Cheeseman, J. R.; Keith, T.; Petersson, G. A.; Montgomery, J. A.; Raghavachari, K.; Al-Laham, M. A.; Zakrzewski, V. G.; Ortiz, J. V.; Foresman, J. B.; Cioslowski, J.; Stefanov, B. B.; Nanayakkara, A.; Challacombe, M.; Peng, C. Y.; Ayala, P. Y.; Chen, W.; Wong, M. W.; Andres, J. L.; Replogle, E. S.; Gomperts, R.; Martin, R. L.; Fox, D. J.; Binkley, J. S.; Defrees, D. J.; Baker, J.; Stewart, J. J. P.; Head-Gordon, M.; González, C.; Pople, J. A. GAUSSIAN 94, Gaussian, Inc., Pittsburgh, PA, 1995. (c) González, C.; Schlegel, H. B. *J. Chem. Phys.* **1989**, *90*, 2154. (d) González, C.; Schlegel, H. B. *J. Phys. Chem.* **1990**, *94*, 5523.

(13) (a) The DFT calculations were carried out with the three-parameter hybrid method of Becke.^{13b–d} The exchange functional is a combination of local spin density, Hartree–Fock, and Becke-88 functionals.^{13b} The correlation functional is a combination of the Lee–Yang–Parr^{13c} gradient corrected correlation functional and Vosko–Wilk–Nusair^{13d} local correlation functional. (b) Becke, A. D. *Phys. Rev. A* **1988**, *37*, 78. (c) Becke, A. D. *J. Chem. Phys.* **1993**, *98*, 5648. (d) Stevens, P. J.; Devlin, F. J.; Chablowski, C. F.; Frisch, M. J. *J. Phys. Chem.* **1994**, *80*, 11623. (e) Lee, C.; Yang, W.; Parr, R. G.; Frisch, M. J. *Phys. Rev.* **1988**, *B41*, 785. (f) Vosko, S. H.; Wilk, L.; Nusair, M. *Can. J. Phys.* **1980**, *58*, 1200.

(14) Bach, R. D.; Glukhovtsev, M. N.; Gonzalez, C. Marquez, M.; Estévez, C. M.; Baboul, A. G.; Schlegel, H. B. *J. Phys. Chem.* (in press).

(15) Yamabe, S.; Kondou, C.; Minato, T. *J. Org. Chem.* **1996**, *61*, 616.

Table 1. Total and Relative Energies (in parentheses) for the Epoxidation of Ethene by Peroxyformic Acid in the Gas Phase^a

computational level	HCOOOH	ethene	cluster-1	TS-2
MP2/6-31G(d)//MP2/6-31G(d)	-264.187820	-78.294286	-342.488965 (-4.3)	-342.455882 (16.5)
B3LYP/6-311G(d,p)//B3LYP/6-311G(d,p)	-264.963266	-78.613977	-343.581636 (-2.8)	-343.553521 (14.9)
QCISD(T)/6-31G(d)//QCISD/6-31G(d) ¹⁴	-264.211180	-78.322230	-	-342.503382 (18.8)

^a Total energies are in Hartrees; relative energies (in kcal mol⁻¹) are computed from isolated reactants.

(d), and BD(T)/6-31G(d)//QCISD(T)/6-31G(d), although the transition structure geometries for the neutral reaction calculated at these levels of theory are in good agreement.^{14,17} The B3LYP DFT method has also been shown to underestimate the central barrier for gas-phase S_N2 reactions.¹⁶ Transition structures for the epoxidation of ethene and of a series of substituted and delocalized alkenes computed with the B3LYP method are in remarkably close agreement with transition structures fully optimized at the QCISD and CCSD(T) levels.¹⁴ However, delocalized structures like 1,3-butadiene exhibit an unsymmetrical approach of the oxygen at the MP2, B3LYP, and QCISD levels of theory.¹⁷ These transition structures bear a remarkable resemblance to that proposed by Hanzlik for a styrene derivative on the basis of a secondary kinetic isotope effect.¹⁸

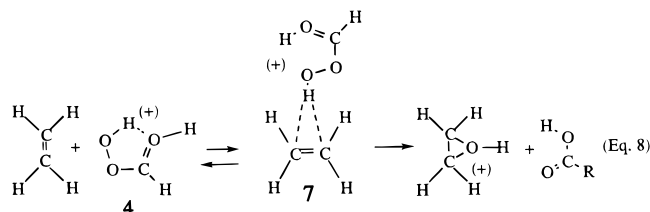
Classical activation barriers (ΔE^\ddagger) for ethene epoxidation with peroxyformic acid are predicted to be 19.4 and 18.8 kcal mol⁻¹ at the CCSD(T)/6-31G(d)//CCSD(T)/6-31G(d) and QCISD(T)/6-31G(d)//QCISD/6-31G(d) levels, respectively.¹⁴ The classical barriers (Table 1) are computed from the isolated reactants since the free energy of formation of gas phase cluster-1 of ethene and peroxyformic acid is positive at the B3LYP/6-311G(d,p) level as a consequence of a fairly large negative entropy of reaction ($\Delta G_{298} = 5.1$ kcal mol⁻¹, $\Delta H_{298} = -1.6$ kcal mol⁻¹, $\Delta S_{298} = -22.4$ cal mol⁻¹ K⁻¹, Figure 2). A second but equally significant facet of TS-2 is the position of the peroxy acid hydrogen in the transition structure. The relatively small experimental kinetic isotope effect ($k_H/k_D = 1.17$) reported for alkene epoxidation¹⁸ is consistent with minimal proton transfer in the TS. We compute an O₃-H₇ bond distance of 1.003 Å in TS-2 and consequently the proton transfer takes place after the barrier is crossed. The obligatory charge separation attending heterolytic O-O bond breaking is partially abated by this 1,4-hydrogen shift that affords a neutral carboxylic acid leaving group. It is this intramolecular neutralization of charge that renders a peroxy acid such an effective oxygen atom donor.

Since these epoxidation reactions are typically associated with negative entropies of activation,¹⁹ the $-T\Delta S_{298}^\ddagger$ term cannot be neglected, and the relative reactivities are best expressed in terms of free energies of activation. For the neutral parent reaction with ethene the classical barrier at the B3LYP/6-311G(d,p) level is predicted to be 14.9 kcal mol⁻¹ (TS-2, Figure 2, $\Delta G_{298}^\ddagger = 25.7$ kcal mol⁻¹, $\Delta H_{298}^\ddagger = 14.8$ kcal mol⁻¹, $\Delta S_{298}^\ddagger = -36.3$ cal mol⁻¹ K⁻¹). These findings are consistent with the magnitude of the pseudo-first-order rate constant given by Kropf^{20a,b} for the epoxidation of ethene by peroxyacetic acid at 19.5 °C in

dichloromethane solvent. From experimental studies it is evident that MCPBA epoxidation of alkenes is subject to general acid catalysis and that acids that are strong enough to give meaningful rate increases may also destroy the epoxide product. It now remains to find an explanation for the meager role of protic acid catalysis in alkene epoxidation.

The site of protonation of the peracid functionality is a first objective that must be resolved. Protonation of both the carbonyl oxygen (O₃, Figure 3) and the incipient carboxylate oxygen (O₂) is possible. At the MP2/6-31G(d) level of theory we predict that the energy minimum structure for peroxyformic acid **3** protonated on the carbonyl oxygen has the peroxy acid in its anti conformation (**4**, Figure 3). We also located structure **5** that was also protonated on O₃ but in the typical cyclic hydrogen bonded structure. We suggest that global minimum **4** is more stable than **5** by 11.9 kcal mol⁻¹ because of the hydrogen bonding interaction of the more acidic hydrogen on O₃ with the terminal oxygen atom (O₁). Protonation on O₂ provided a minimum **6** that is 31.7 kcal mol⁻¹ higher in energy reflecting the loss in hydrogen bonding.

We next examined the magnitude of the activation barrier for oxygen atom transfer from protonated peroxyformic acid **4** to ethene (eq 8).



As anticipated the classical barrier height computed from cluster **7** for the formal transfer of HO⁺ to ethene affording protonated oxirane is only 6.8 kcal mol⁻¹ (TS-8a, Figure 4) at the MP2/6-31G(d) level. The reactant cluster **7** between ethene and protonated peroxy acid **4** is stabilized by 14.2 kcal mol⁻¹. The relatively low activation barrier is consistent with a very early transition structure for this highly exothermic reaction ($\Delta E = -61.7$ kcal mol⁻¹ at the MP2/6-31G(d) level) and the C₂-H₉ distance of 2.285 Å reflects the acid-base interaction of the alkene π -system with the protonated peracid **4**. We have shown that TS-8a is connected to kinetic products protonated oxirane and formic acid (eq 8) by the intrinsic reaction coordinate^{12c,d} (IRC).

At the B3LYP/6-311G(d,p) level **7** is 13.2 kcal mol⁻¹ lower in energy relative to its isolated reactants ($\Delta G_{298} = -3.6$ kcal mol⁻¹) and the classical barrier for hydroxylation of ethene is -8.8 kcal mol⁻¹. The corresponding barrier computed from cluster **7** for ethene oxidation is

(16) Glukhovtsev, M. N.; Bach, R. D.; Pross, A.; Radom, L. *Chem. Phys. Lett.* **1996**, *260*, 558.

(17) Bach, R. D.; Glukhovtsev, M. N.; Canepa C. *J. Am. Chem. Soc.*, submitted.

(18) Hanzlik, R. P.; Shearer, G. O. *J. Am. Chem. Soc.* **1975**, *106*, 1401.

(19) Hoveyda, A. H.; Evans, D. A.; Fu, G. C. *J. Chem. Rev.* **1993**, *93*, 1307.

(20) (a) Kropf, H.; Yazdanbachs, M. R. *Tetrahedron* **1974**, *30*, 3455. (b) A pseudo-first-order rate constant of 1.92×10^{-6} s⁻¹ has been reported. Assuming a tenfold excess concentration of ethene with respect to peroxyacetic acid, a second-order rate constant of 1.92×10^{-5} M⁻¹ s⁻¹ can be calculated and a $\Delta G_{298}^\ddagger = 25.3$ kcal mol⁻¹ may be derived using standard nonvariational transition state theory.

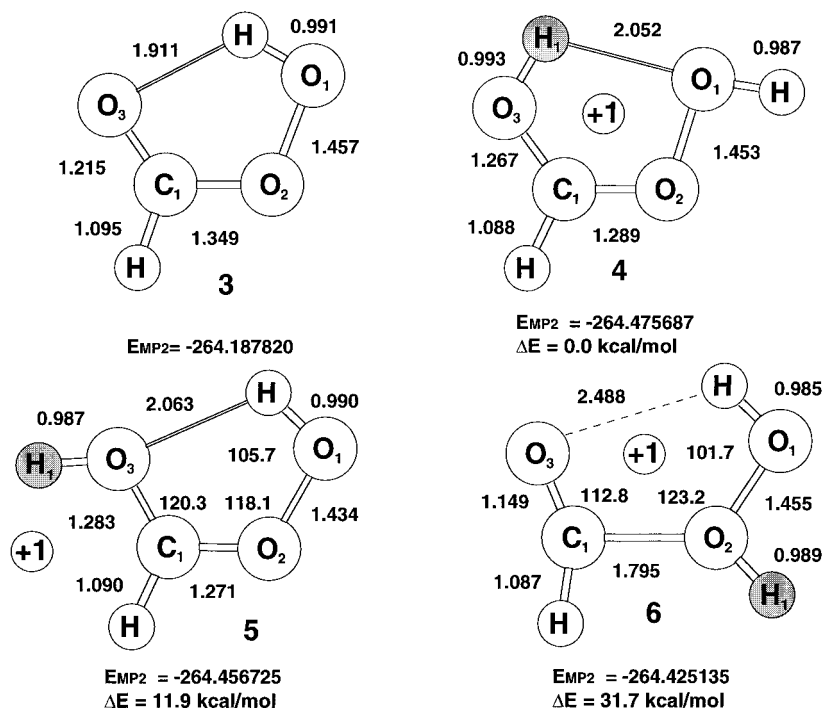


Figure 3. Peroxyformic acid (3) and three protonated structures (4–6). Geometries are at MP2(full)/6-31G(d). Total energies are in Hartrees, distances in angstroms, and angles in degrees.

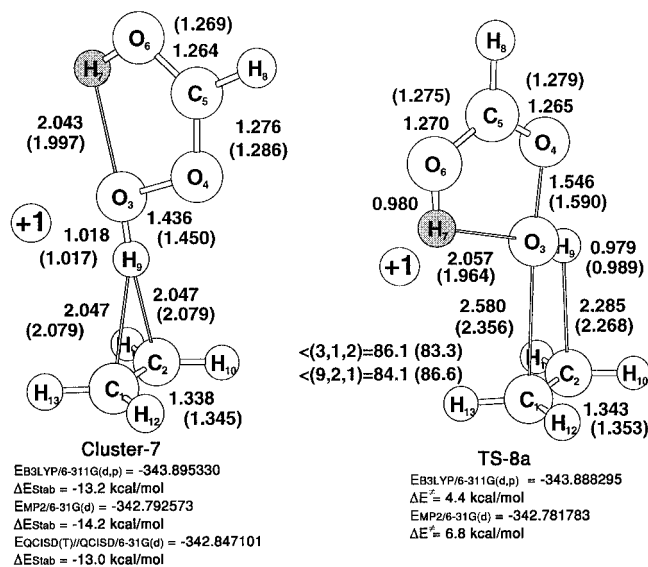


Figure 4. Protonated peroxyformic acid cluster with ethylene (7) and transition structure (TS-8a) with a planar reaction site geometry optimized at B3LYP/6-311G(d,p). Total energies are in Hartrees, distances in angstroms, and angles in degrees. The total energy of protonated peroxyformic acid at the level indicated is -265.260253 Hartrees. The stabilization energy for 7 is relative to isolated reactants, and the activation energy for TS-8a is relative to cluster 7. Geometrical parameters optimized at the MP2/6-31G(d) level are given in parentheses.

4.4 kcal mol⁻¹ (TS-8a). The free energy of activation is dramatically reduced with respect to the parent neutral reaction of eq 7 ($\Delta G_{298}^\ddagger = 3.5$ kcal mol⁻¹, $\Delta H_{298}^\ddagger = 3.3$ kcal mol⁻¹, $\Delta S_{298}^\ddagger = -0.7$ cal mol⁻¹ K⁻¹) when the activation parameters are computed from reactant cluster 7. The $\Delta\Delta G_{298}^\ddagger$ of -22.1 kcal mol⁻¹ for the protonated versus neutral oxidative reactions is consistent with experimental observations noted above for protonated hydrogen peroxide. In this instance both DFT and MP2 methods give remarkably close agreement for geometries

and energetics. The nature of the transition structure for oxidation with protonated peroxyformic acid differs markedly from the symmetrical approach of the unprotonated peroxyformic acid in spiro TS-2 (Figure 2). As noted¹⁴ for the approach of the peroxy acid in the parent reaction (eq 7) the potential energy surface is very shallow and a geometrically constrained spiro second-order saddle point is only 0.3 kcal mol⁻¹ higher in energy than the first-order saddle point TS-8a.

As a consequence of our earlier difficulties with symmetrical versus unsymmetrical geometries found for epoxidation under neutral conditions at the MP2 level,¹⁴ the transition structure for the acid-catalyzed epoxidation of ethene has been recomputed at the QCISD/6-31G(d) level of theory. At this higher correlated level the stabilization energy of cluster 7 relative to its isolated reactants is -13.0 kcal mol⁻¹ (Table 2, Figure 4). When the QCISD transition structure geometry optimization was started at the planar DFT geometry (H₉-O₃-C₁-C₂ = 1.5°), the protonated peroxy acid 4 slowly moved toward a spiro orientation. When the dihedral angle H₉-O₃-C₁-C₂ was 68.6°, the difference in energy between this structure and a constrained spiro TS (H₉-O₃-C₁-C₂ = 90°) was only 0.3 kcal mol⁻¹. The resulting classical barrier for the fully optimized TS-8b is only 6.4 kcal mol⁻¹ (QCISD(T)//QCISD/6-31G(d)) when computed from cluster 7 (Figure 5). More significantly, the potential energy surface for torsional motion of the protonated peroxyformic acid at all the three levels of theory is very shallow. Thus it appears that the difficulties encountered at the MP2 and DFT levels in arriving at the proper symmetrical spiro geometry are alleviated at the higher correlated QCISD level. The O-O elongation in TS-2 and TS-8b at the QCISD/6-31G(d) level are 0.43 and 0.11 Å, respectively, reflecting the relative positions along the reaction coordinate for oxygen transfer.

Assuming that the catalytic activity is ascribed to protonation of the peracid, the overall rate expression for alkene epoxidation in the presence of strong acid (eq 9)

Table 2. Total and Relative Energies (in parentheses) for the Epoxidation of Ethene by Protonated Peroxyformic Acid in the Gas Phase^a

computational level	H(C=OH)OOH ⁺	cluster-7	TS-8
MP2/6-31G(d)//MP2/6-31G(d)	-264.475687	-342.792573 (-14.2)	-342.781783 (-7.4)
B3LYP/6-311G(d,p)//B3LYP/6-311G(d,p)	-265.260253	-343.895330 (-13.2)	-343.888295 (-8.8)
QCISD(T)/6-31G(d)//QCISD/6-31G(d)	-264.504172	-342.847101 (-13.0)	-342.836924 (-6.6)

^a Total energies are in Hartrees; relative energies (in kcal mol⁻¹) are computed from isolated reactants.

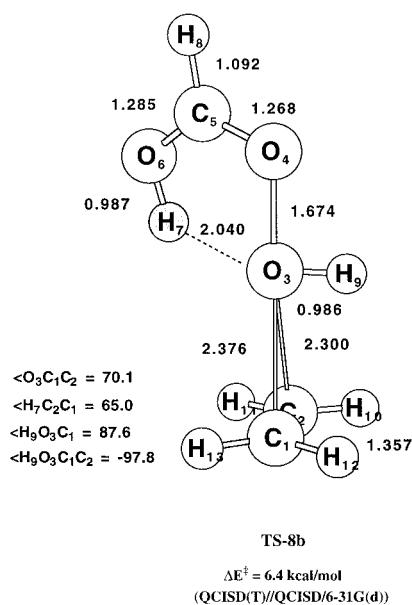


Figure 5. Transition structure with a spiro geometry of the reaction side optimized at the QCISD/6-31G(d) level. The total energy calculated at the QCISD(T)//QCISD/6-31G(d) level is -342.83692 Hartrees. Distances are shown in angstroms and bond angles are in degrees. The classical barrier (ΔE^\ddagger) is computed relative to cluster 7.

would be the sum of an unprotonated (k_0) and a protonated peroxy acid component (k_{cat}). A similar rate expression was derived for the oxidation of sulfides.^{9a} The

$$-\frac{d[\text{peracid}]}{dt} = k_0[\text{alkene}][\text{peracid}] + k_{\text{cat}}[\text{alkene}][\text{peracid}^+] \quad (\text{eq } 9)$$

theoretical results clearly show that the rate constant for the catalyzed reaction, k_{cat} , would be many orders of

Table 3. Total and Relative Energies (in parentheses) for the Epoxidation of Ethene by Peroxyformic Acid Complexed to HF^a

computational level	cluster-9	TS-10
MP2/6-31G(d)//MP2/6-31G(d)	-364.386224	-442.658096 (14.1)
B3LYP/6-311G(d,p)//B3LYP/6-311G(d,p)	-365.446912	-444.042591 (11.5)

^a Total energies are in Hartrees; relative energies (in kcal mol⁻¹) are computed from ethylene and cluster-9

magnitude greater than k_0 . In this hypothesis the concentration of protonated peroxy acid ([peracid⁺]) becomes a controlling factor. However, our best estimate is that the concentration of protonated MCPBA in a relatively nonpolar solvent like benzene is too low to have a measurable affect upon the rate of epoxidation. The effective acidity of trifluoroacetic acid, i.e. its ability to protonate peroxybenzoic acid, was shown earlier to be dependent on both the solvent and the presence of benzoic acid.^{9a}

This prompted us to examine the role of an undissociated acid (HA) in this reaction. We chose hydrofluoric acid as a model acid and find that the stabilization energy for formation of reactant cluster **9** is -8.7 kcal mol⁻¹ at the B3LYP/6-311G(d,p) level (Table 3, Figure 6). The barrier height for ethene epoxidation with the HCO₃H·HF complex is predicted to be 11.5 kcal mol⁻¹ (TS-10, $\Delta H^\ddagger_{298} = 11.6$ kcal mol⁻¹, $\Delta S^\ddagger_{298} = -36.4$ cal mol⁻¹ K⁻¹, $\Delta G^\ddagger_{298} = 22.4$ kcal mol⁻¹). This constitutes a reduction in free energy of activation of 3.4 kcal mol⁻¹ with respect to the uncatalyzed pathway that is consistent with our kinetic data. The extent of O–O bond elongation (0.406 Å) is only slightly smaller than that for TS-2. We also did observe reasonable agreement with the activation barrier computed at the MP2/6-31G(d) level ($\Delta E^\ddagger = 14.1$ kcal mol⁻¹). However, as noted above, the MP2 method

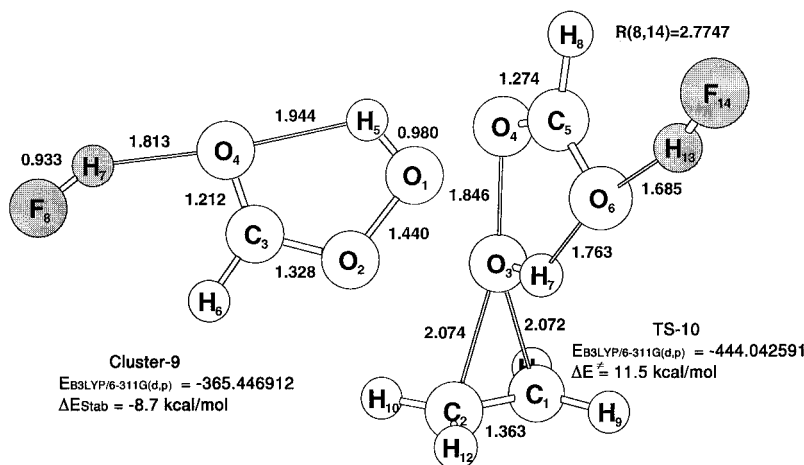


Figure 6. Peroxyformic acid–hydrogen fluoride cluster (**9**) and its transition structure for reaction with ethylene (TS-10). Geometries are at B3LYP/6-311G(d,p). The stabilization energy for **9** is relative to isolated reactants, and activation energy for TS-10 is relative to cluster **9** and ethylene. Total energies in Hartrees, distances in angstroms, and angles in degrees. The total energy of hydrogen fluoride at the level indicated is -100.469728.

suggested an unsymmetrical approach of oxygen to the carbon-carbon double bond ($O_3-C_1 = 2.240 \text{ \AA}$, $O_3-C_2 = 1.842 \text{ \AA}$).

These data are consistent with the rate expression given in eq 10 where K_{eq} is the equilibrium constant for formation of a reactant cluster corresponding to **9**. Equation 10 has the same form as the empirically derived eq 6, but k_{HA} is now resolved in the product of the rate constant for the catalyzed process (k_{cat}) and the equilibrium constant for the formation of the cluster (K_{eq}). If

$$-\frac{d[\text{peracid}]}{dt} = k'_2[\text{alkene}][\text{peracid}] \text{ with } k'_2 = k_0 + k_{cat}K_{eq}[\text{HA}] \text{ (eq 10)}$$

the alkene substrate is also capable of complexation with HA, then a decrease in rate would be expected, as noted above for ethyl crotonate.^{3b}

Conclusions

(a) The predicted activation barrier for epoxidation of ethene with fully protonated peroxyformic acid (TS-**8a**) is indeed quite low ($\Delta E^\ddagger = 6.4 \text{ kcal mol}^{-1}$). However, under typical reaction conditions in nonpolar solvents, an effective concentration of protonated peroxy acid is not attainable, and the stability of the product epoxide is in question. At the same level of theory (QCISD(T)/6-31G(d)//QCISD/6-31G(d)) the barrier of the uncatalyzed reaction is $18.8 \text{ kcal mol}^{-1}$.

(b) The increase in rate of alkene epoxidations observed upon addition of carboxylic acids of moderate acidity has been rationalized in terms of a preequilibrium forming a reactant cluster between the peroxy acid and the catalyst (HA) as exemplified in eq 10. The hydrogen bond between HA and the peroxy acid, activating the latter, is capable of lowering the barrier for epoxidation of ethene by peroxyformic acid by about 3 kcal mol^{-1} (TS-**10**) with respect to the uncatalyzed process.

(c) While the B3LYP/6-311G(d,p) level affords good geometries for alkene epoxidation with neutral peroxy acids, the dihedral angle between the two planes of the reactants differ by 90° when compared at the QCISD level. The reaction surface for approach of both neutral and protonated peroxy acid to the carbon-carbon double bond is extremely shallow at all levels of theory examined.

Acknowledgment. This work was supported in part by the National Science Foundation (CHE-9531242) and a NATO Collaborative Research Grant (900707). We are also thankful to the National Center for Supercomputing Applications (Urbana, Illinois) and the Pittsburgh Supercomputing Center for generous amounts of computer time. Carlo Canepa wishes to thank the Università di Torino, Italy, that has made possible his stay at the University of Delaware.

JO950930E